

AD-A052 062

AEROSPACE CORP EL SEGUNDO CALIF MATERIALS SCIENCES LAB F/G 11/6
TRANSVERSE FRACTURE BEHAVIOR OF GRAPHITE-ALUMINUM COMPOSITES.(U)
MAR 78 M F AMATEAU, D L DULL F04701-77-C-0078

UNCLASSIFIED

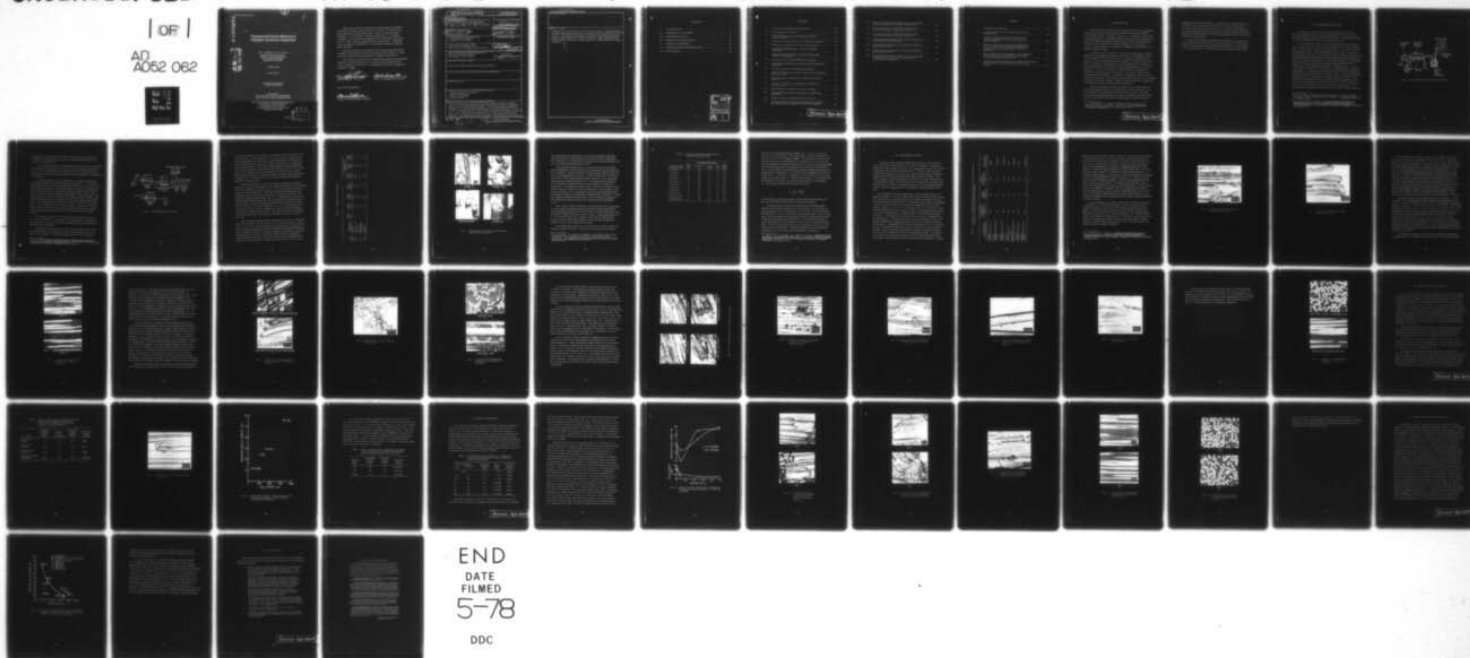
TR-0078(3726-03)-1

SAMSO-TR-78-69

NL

| OF |

AD
A052 062





AD A 052062

AD No.
DDC FILE COPY

Transverse Fracture Behavior of Graphite-Aluminum Composites

M. F. AMATEAU and D. L. DULL
Materials Sciences Laboratory
The Ivan A. Getting Laboratories
The Aerospace Corporation
El Segundo, Calif. 90245

15 March 1978

Interim Report

APPROVED FOR PUBLIC RELEASE;
DISTRIBUTION UNLIMITED

Prepared for
NAVAL SURFACE WEAPONS CENTER
White Oak, Silver Spring, Maryland 20910

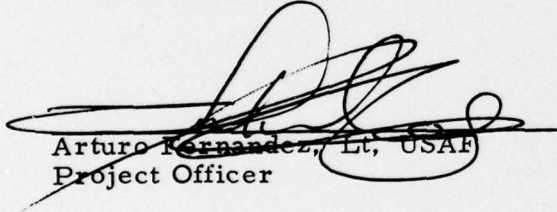
SPACE AND MISSILE SYSTEMS ORGANIZATION
AIR FORCE SYSTEMS COMMAND
Los Angeles Air Force Station
P.O. Box 92960, Worldway Postal Center
Los Angeles, Calif. 90009



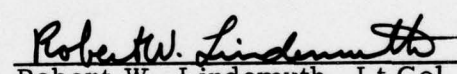
This interim report was submitted by The Aerospace Corporation, El Segundo, CA 90245, under Contract No. F04701-77-C-0078 with the Space and Missile Systems Organization, Deputy for Advanced Space Programs, P. O. Box 92960, Worldway Postal Center, Los Angeles, CA 90009. It was reviewed and approved for The Aerospace Corporation by W. C. Riley, Director, Materials Sciences Laboratory. Lieutenant Arturo Fernandez, SAMSO/YCPT, was the project officer for Advanced Space Programs.

This report has been reviewed by the Information Office (OI) and is releasable to the National Technical Information Service (NTIS). At NTIS, it will be available to the general public, including foreign nations.

This technical report has been reviewed and is approved for publication. Publication of this report does not constitute Air Force approval of the report's findings or conclusions. It is published only for the exchange and stimulation of ideas.



Arturo Fernandez, Lt, USAF
Project Officer



Robert W. Lindemuth, Lt Col, USAF
Chief, Technology Plans Division

FOR THE COMMANDER



Floyd R. Stuart, Colonel, USAF
Deputy for Advanced Space Programs

UNCLASSIFIED

SECURITY CLASSIFICATION OF THIS PAGE (When Data Entered)

19 REPORT DOCUMENTATION PAGE		READ INSTRUCTIONS BEFORE COMPLETING FORM	
1. REPORT NUMBER	2. GOVT ACCESSION NO.	3. RECIPIENT'S CATALOG NUMBER	
18 SAMS0 TR-78-69			
4. TITLE (and Subtitle)		5. TYPE OF REPORT & PERIOD COVERED	
6 TRANSVERSE FRACTURE BEHAVIOR OF GRAPHITE-ALUMINUM COMPOSITES.		9 Interim report	
7. AUTHOR(s)		8. PERFORMING ORG. REPORT NUMBER	
10 Maurice F. Amateau Dennis L. Dull		14 TR-0078(3726-03)-1	
		9. CONTRACT OR GRANT NUMBER(s)	
		15 F04701-77-C-0078	
9. PERFORMING ORGANIZATION NAME AND ADDRESS		10. PROGRAM ELEMENT, PROJECT, TASK AREA & WORK UNIT NUMBERS	
The Aerospace Corporation El Segundo, Calif. 90245			
11. CONTROLLING OFFICE NAME AND ADDRESS		12. REPORT DATE	
Naval Surface Weapons Center White Oak, Silver Spring, Maryland 20910		11 15 March 1978	
		13. NUMBER OF PAGES	
		59 42 58P	
14. MONITORING AGENCY NAME & ADDRESS (if different from Controlling Office)		15. SECURITY CLASS. (of this report)	
Space and Missile Systems Organization Air Force Systems Command Los Angeles, Calif. 90009		Unclassified	
		15a. DECLASSIFICATION/DOWNGRADING SCHEDULE	
16. DISTRIBUTION STATEMENT (of this Report)			
Approved for public release; distribution unlimited.			
17. DISTRIBUTION STATEMENT (of the abstract entered in Block 20, if different from Report)			
18. SUPPLEMENTARY NOTES			
19. KEY WORDS (Continue on reverse side if necessary and identify by block number)			
Graphite-Aluminum Composites Composite Processing Transverse Strength Fracture Modes			
20. ABSTRACT (Continue on reverse side if necessary and identify by block number)			
A determination was made of the transverse tensile strength of graphite-aluminum composites produced from various fiber and matrix compositions and by a variety of processing methods. Processing methods included the standard Ti-B chemical vapor deposition process and modifications to that process, the sodium process, and the nickel-coated fiber method. Precursor rayon, pitch, high-modulus polyacrylonitrile (PAN) and low-modulus PAN fibers were investigated, as well as 201, 6061, and 1100 aluminum-alloy matrices. The transverse fracture strength is influenced by the processing			

DD FORM 1473
(FACSIMILE)

403 644

JOB

UNCLASSIFIED

SECURITY CLASSIFICATION OF THIS PAGE (When Data Entered)

UNCLASSIFIED

SECURITY CLASSIFICATION OF THIS PAGE(When Data Entered)

19. KEY WORDS (Continued)

20. ABSTRACT (Continued)

method and the type of fiber but not by the matrix alloy. Those processes and fibers that promote fiber-matrix reaction result in the highest transverse strength. The fractured surfaces, as examined by scanning electron microscopy, revealed fiber-matrix separation and fiber pullout as the dominant features of low-transverse-strength composites. Fiber splitting and the absence of fiber pullout were characteristic of the high-transverse-strength composites.

UNCLASSIFIED

SECURITY CLASSIFICATION OF THIS PAGE(When Data Entered)

CONTENTS

I.	INTRODUCTION	7
II.	EXPERIMENTAL METHODS	9
III.	PROCESSING EFFECTS	19
IV.	FIBER AND MATRIX EFFECTS	39
V.	THERMAL TREATMENTS	45
VI.	FIBER FRACTION AND DISTRIBUTION	55
VII.	CONCLUSIONS	59

ACCESSION for	
DTIC	White Section <input checked="" type="checkbox"/>
DDI	Duty Section <input type="checkbox"/>
UNANNOUNCED	<input type="checkbox"/>
JUSTIFICATION.....	
BY.....	
DISTRIBUTION/AVAILABILITY CODES	
Dist.	AVAIL. and/or SPECIAL
A	

FIGURES

1.	Ti-B Chemical Vapor Deposition Process	10
2.	Electrodeposition Process	12
3.	Characteristic Cross-Sectional Shapes of Fibers Used in the Study	15
4.	Transverse Fracture Surface of T 50/201 (S) Composite	22
5.	Brittle Layer Attached to Ductile Aluminum Matrix	23
6.	Longitudinal Metallographic Sections of T 50/201 Composites	25
7.	Transverse Fracture Surface of Sodium-Processed T 50/201 (N) Composite	27
8.	Fracture Surface of HM 1000/201 (P) Composite	28
9.	Longitudinal and Transverse Sections of HM 1000/201 (P) Composite	29
10.	Fracture Surfaces of T 300/201 (S) Composite	31
11.	Adherence of Material to Surface of Fiber on T 300/201 (S) Fracture Surface	32
12.	Clean Appearance of Fibers on T 300/201 (C) Fracture Surface	33
13.	Coating on T 300 Fibers Pulled From T 300/201 (C) Fracture Surface	34
14.	Fiber Pullout on T 300/201 (C) Fracture Surface	35
15.	Longitudinal and Transverse Sections of T 300/201 (C) Composite	37
16.	Fracture Surface of HM 3000/201 (S) Composite	41
17.	Relationship Between Carbide Formation and Transverse Strength of Various Graphite Fiber/201 (S) Composites	42

Preceding Page BLANK

18.	Effect of Thermal Treatments on Transverse Strength and Matrix Hardness of T 50/201 (S) Composite	47
19.	Fracture Surface of T 50/201 (S) Composite Heat Treated Near Solidus Temperature for 4.5 hr	48
20.	Fracture Surface of T 50/201 (S) Composite Heat Treated Near Solidus Temperature for 24 hr	49
21.	Longitudinal Fiber Splitting in T 50/201 (S) Composite Heat Treated at 571°C for 48 hr	50
22.	Longitudinal Cross Section of T 50/201 (S) Composite Heat Treated at 571°C	51
23.	Transverse Cross Section of T 50/201 (S) Composite Heat Treated at 571°C	52
24.	Composite Fiber Fraction Versus Transverse Strength, Plotted Without Regard to Processing Method or Local Fiber Concentrations	56

TABLES

1.	Graphite Fiber Properties	14
2.	Composite Materials Fabricated for Transverse Strength Study	17
3.	Transverse Strength and Fracture Behavior of Graphite-Aluminum Composites Processed by Various Methods	20
4.	Effect of Fiber Type on Transverse Strength and Fracture Behavior of Graphite/201 Matrix-Alloy Composites Processed by Standard Ti-B CVD Method (S)	40
5.	Effect of Matrix-Alloy Composition on Strength and Fracture Behavior of HM 3000/Aluminum-Alloy Composites Produced by S Process	43
6.	Transverse Fracture Behavior of T 50/201 (S) Composites Heat Treated To Produce Additional Fiber-Matrix Reaction	45

I. INTRODUCTION

Graphite-aluminum composites potentially offer a unique combination of high specific strength and modulus, moderate temperature stability, excellent fabricability, joinability, and low cost. In addition to these basic structural properties, the graphite-aluminum composites also possess such useful mechanical and physical properties as high electrical and thermal conductivity, low coefficient of thermal expansion, low coefficient of friction, relatively good wear resistance, antigalling characteristics, and excellent fatigue strength.

At present, the major obstacle to achieving a wide range of efficient applications for graphite-aluminum composites is the disappointing transverse strength of this class of materials. Although crossplying the composites to achieve off-axis properties is possible, as is done with the resin matrix composites, considerable structural advantage will be realized if the composites are used primarily in the unidirectional form, as is boron-aluminum. In those cases where crossplied layups are advantageous, additional transverse strength will result in even greater efficiency and composite design versatility. In addition to crossplying, other techniques that result in a dilution of the fiber fraction can also be effective in increasing structural transverse strength.¹ Higher intrinsic transverse strength will allow these techniques to be applied more effectively.

There are a number of possible reasons for the limited transverse strength of graphite-aluminum composites, but the most likely one is the poor strength of the bond between the fiber and the matrix. The most successful processing methods used to produce graphite-aluminum composites are those that limit the fiber-matrix reaction in order to prevent

¹ J. F. Dolowy and B. A. Webb, "Failure Processes in Cross-Ply Graphite-Aluminum Composites," Submitted to Failure Modes and Processing of Composites, IV, AIME, New York.

degradation of the fiber properties. The diameter of graphite fibers is 10 to 20 times finer than that of boron fibers. Therefore, unlike boron-aluminum processing methods, which achieve transverse strength by permitting a reasonable degree of fiber-matrix reaction, graphite-aluminum processing methods restrict the amount of permissible reaction to that just sufficient to cause wetting.

Variations in processing methods should result in variations in the fiber-matrix reactions and, hence, transverse strength. In this study, a number of standard processing methods and variations in these methods were examined in order to determine the extent and nature of this effect.

II. EXPERIMENTAL METHODS

Three different methods of composite processing were used to produce graphite-aluminum materials in this study: the Ti-B process, the sodium process, and the nickel-plating process. A detailed description of these methods can be found in a recent review article.²

The Ti-B process consists of first codepositing boron and titanium onto the graphite fiber by chemical vapor deposition (CVD) from TiCl_4 and BCl_3 . This process, referred to as the standard Ti-B process, is shown schematically in Fig. 1 and is designated S in this report. Two modifications of this process were used to produce different interface characteristics. Scanning Auger microprobe analysis revealed that oxygen was a ubiquitous species at the fracture interface of S-processed materials.³ In an attempt to alter this characteristic, the fiber was hydrogen precleaned at the beginning of the coating processes within the coating reactor, i.e., prior to the standard CVD process. Composites processed by this technique are designated H. Composites produced by the H process were obtained from Materials Concepts Incorporated, Columbus, Ohio. In another modification of the S process, the fibers are precoated with pyrolytic carbon. This process is particularly effective in protecting the low-modulus polyacrylonitrile (PAN)-based fibers, such as Thornel 300 (T 300), to permit subsequent metal infiltration without serious property degradation. This pretreatment was applied to two different types of fiber by Fiber Materials

²M. F. Amateau, "Progress in the Development of Graphite-Aluminum Composites Using Liquid Infiltration Technology," J. Compos. Mater. **10**, 279 (October 1976).

³D. L. Dull and M. F. Amateau, Transverse Strength Properties of Graphite-Aluminum Composites, Quarterly Progress Report No. 1, TOR-0077(2726-03)-1, The Aerospace Corporation, El Segundo, California (10 January 1977).

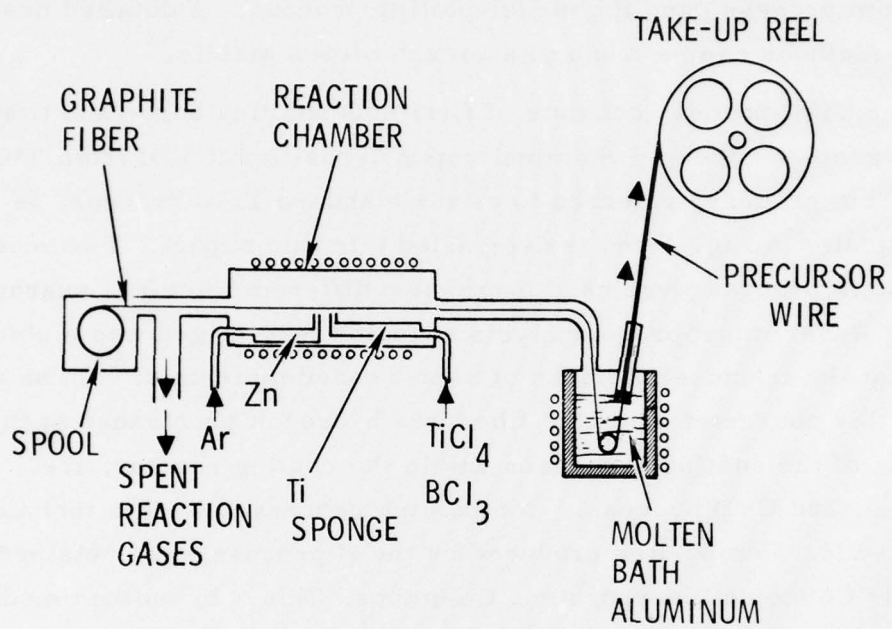


Fig. 1. Ti-B Chemical Vapor Deposition Process

Incorporated. These fibers were subsequently infiltrated by Materials Concepts Incorporated by the S process. Composites produced by this technique are designated C.

In the sodium process, the graphite fibers are treated in liquid sodium at 550°C and then immersed in, first, a tin-2% magnesium bath at 600°C and, then, a molten aluminum alloy bath at 20 to 50°C above the liquidus. This process, which has been described in detail by Goddard,⁴ is designated N in this report.

The nickel-plating process, designated P, consists of infiltrating nickel-plated fibers directly with molten aluminum alloy. The method for precoating the fibers is shown schematically in Fig. 2. Any sizing or other surface film that may be on the graphite fibers is removed by drawing the fibers through a furnace containing an argon atmosphere heated to 580°C. The fibers are then woven through a glass ladder, which spreads them and directs them into an electrolyte bath that contains a solution of NiSO_4 and NiCl_2 (Watts bath) at room temperature. Pure nickel anodes surround the fibers. Electrodeposition is carried out at 4 to 6 V. The current ranges from 3 to 5 A, depending on the number of fibers. The fibers are drawn into a water rinse bath and then into an alcohol rinse bath prior to being drawn through a drying furnace at 125°C in which argon is continually passing.

The composite product of each of the processing methods is a wire 0.5 to 1 mm in diameter. These wires were subsequently consolidated into plates 2- to 3-mm thick by diffusion bonding, which was performed at DWA Composite Specialties.

Four different fiber types were used in the composites; each represented a different currently available commercial precursor form, e.g., rayon, PAN, and pitch. Both high-modulus (Type I) and low-modulus

⁴D. M. Goddard, Interface Reactions During Preparation of Aluminum-Matrix Composites by the Sodium Process, ATR-77(8162)-3, The Aerospace Corporation, El Segundo, California (20 July 1977).

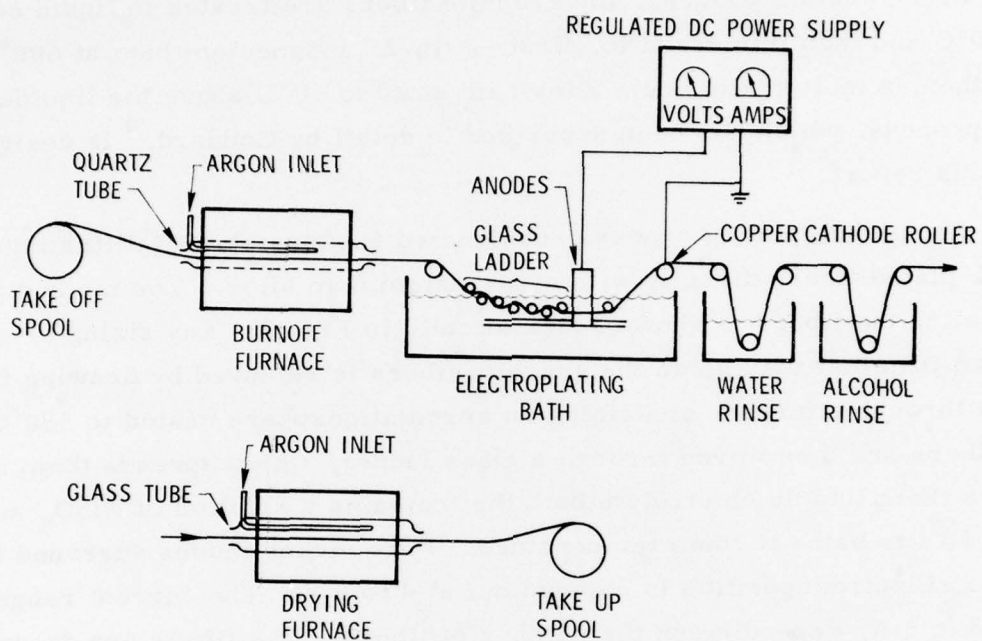


Fig. 2. Electrodeposition Process

(Type II) PAN fibers were included. These fibers and their properties are listed in Table 1. The Thornel 50 (T 50), Thornel Type P (Type P), and Hercules HM 3000 (HM 3000) fibers are highly graphitic, as indicated by the low (0002) d-spacing, and have a larger crystallite size, as indicated by the relatively large x-ray intensity peak height and narrow peak width. These fibers also have a high degree of preferred orientation. The T 300 fiber is less graphitic and has less preferred orientation than the other fibers used in this study. It also has a higher nitrogen content and smaller crystallite size. These differences can result in significantly different infiltration characteristics.

Another characteristic of the fibers that may influence transverse behavior is cross-sectional shape. The significant differences in the various fiber cross sections are shown in Fig. 3. The T 50 fibers have a characteristic crenulated perimeter, resulting from parallel flutes along their length (Fig. 3a). Pitch fibers have either a round cross section or one with a pie-shaped wedge missing (Fig. 3b). The diameters, as well as the extent of this missing wedge, also vary from filament to filament within a typical bundle. The high-modulus HM 3000 fiber has an almost circular cross section and very smooth walls (Fig. 3c). The T 300 cross section varies from almost circular to slightly oval, with many fibers having a distinct kidney-shaped cross section. The walls of this fiber are slightly striated but do not have the deep flutes characteristic of the T 50 fiber (Fig. 3d).

Three different aluminum alloy matrices were chosen for infiltration: 201, 6061, and 1100. The 201 alloy (4.7 Cu, 0.8 Ag, 0.4 Mn, 0.35 Mg, 0.4 Zn, and 0.25 Ti) was selected for this study because it represents the base-line alloy composition; the greatest amount of mechanical properties data on graphite-aluminum composites has been obtained from composites produced with the 201 alloy. This alloy usually results in the highest tensile properties for both the precursor wire and the consolidated plate specimens. The 6061 alloy (1.0 Mg, 0.6 Si, 0.27 Cu, and 0.2 Cr) is a

Table 1. Graphite Fiber Properties

Type	Commercial Designation	Fiber Diameter, μm	Tensile Strength, MPa	Young's Modulus, GPa	Density, g/cm^3 (10^3 kg/m^3)	X-Ray Crystallographic Properties		
						(0002) d-spacing, nm	Relative Peak Height	Relative Peak Width
Rayon	Thornel 50	6	2399	414	1.67	0.342	102	20
Pitch	Thornel Type P (Type P)	8	1209	393	2.00	0.343	241	6
PAN I	Hercules HM 3000 (HM 3000)	7	2270	365	1.81	0.341	100	19
PAN II	Thornel 300 (T 300)	7	2634	241	1.70	0.356	18	68



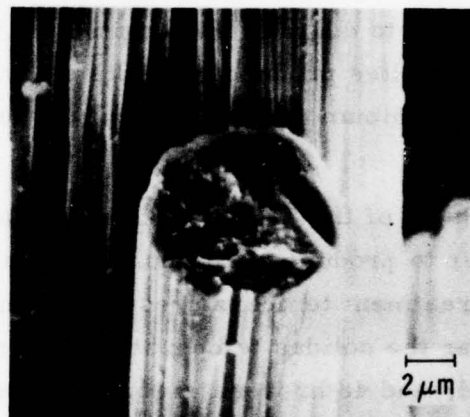
THORNEL 50
a.



THORNEL TYPE P
b.



HERCULES HM 3000
c.



THORNEL 300
d.

Fig. 3. Characteristic Cross-Sectional Shapes of
Fibers Used in the Study

well-characterized wrought alloy for which some composite fabrication experience exists, including both graphite and boron fiber compositions. The 1100 alloy (0.12 Cu) was selected because it is a commercial alloy with one of the highest aluminum contents (99%).

All composites produced for this study, the method of processing, and the parameters used to consolidate the precursor wires into plates are given in Table 2. The fiber fraction of the composites, which is a function of the processing method, fiber type, and alloy composition, varied from 12% to 44%. The Ti-B processed material, either S, H, or C, generally ranges in fiber content from 30% to 40%. The sodium-processed N and the nickel-plated P materials have low fiber fractions, 14% and 12%, respectively. The aluminum carbide (Al_4C_3) content is an indication of the extent of reaction between the fiber and the matrix. When carbide content exceeds 2000 ppm, there is generally sufficient reaction between the fiber and matrix to degrade the longitudinal tensile strength of the fiber.⁵ Among the composites produced for this study, only the T 300/201 (S) material had an aluminum carbide content in the range where fiber degradation occurs.

Some of the T 50/201 (S) material was heat treated after consolidation in order to produce additional reaction between the matrix and the fiber. Heat-treatment temperatures of 571 and 593°C were selected because they are near the solidus temperature of the 201 alloy. Heat-treatment times of 4.5, 24, and 48 hr were used. All heat treatments were performed in vacuum, and the material was allowed to slow cool after the specified number of hours at the designated temperature.

Both longitudinal and transverse tensile tests were performed on the various composite materials. Precursor wire specimens were tensile

⁵W. C. Harrigan, Jr., and D. M. Goddard, "The Effects of Processing Parameters on the Mechanical Properties of Aluminum-Graphite Composites," Proceedings of the 1975 International Conference on Composite Materials, AIME, New York (1975).

Table 2. Composite Materials Fabricated for Transverse Strength Study

Fiber/Matrix Alloy (Processing Method)	Fiber Content, vol%	Consolidation Parameters			Al ₄ C ₃ Content, ppm
		Temperature, °C	Pressure, MPa	Time, min	
T 50/201 (S)	32	570	24	25	1012
T 50/201 (H)	35	574	24	25	1120
T 50/201 (C)	36	568	24	25	480
T 50/201 (N)	14	560	24	25	723
HM 1000/201 (P)	12	568	24	25	778
T 300/201 (S)	36	568	24	25	3280
T 300/201 (C)	44	568	24	25	690
Type P/201 (S)	34	568	24	25	1568
HM 3000/201 (S)	40	568	24	25	369
HM 3000/1100 (S)	30	607	24	30	176
HM 3000/6061 (S)	34	596	24	25	203

tested by the method described by Padilla et al.⁶ The wire specimens were cut to 125-mm lengths, and 660-grit silicon carbide was glued to the ends of the wire over the gripped lengths. The wires were then inserted into the hollow center of braided nylon cord a distance of 50 mm on each end and bonded for a distance of 20 to 25 mm on each side of the gage length. The nylon cord tabs were then gripped about 2 mm above the end of the wire. This method accommodates any extraneous bending of the specimen resulting from misalignment. The tensile load was applied at the rate of 0.008 mm/sec. The cross-sectional area of the composite wire is calculated from the bulk density ρ_f and the linear density λ_f of the fiber; the bulk density of the matrix ρ_m ; and the linear density of the composite λ_c . The average composite cross-sectional area is

$$A_c = \frac{\lambda_f}{\rho_f} + \frac{\lambda_c - \lambda_f}{\rho_m}$$

This method of measuring composite cross section agrees within a few percent of planimeter measurements on photomicrographs.

Transverse tensile tests were performed on consolidated plate material machined into specimens 31.8-mm long by 12.7-mm wide containing a gage section 7.6-mm long by 7.6-mm wide. The specimens are pin loaded with 6.35-mm-diameter pin holes approximately 7 mm from the ends. Aluminum shims were adhesively bonded to the grip ends in order to distribute the load around the pin holes. The specimen was held in a fixture suspended by a steel cable from a test frame to minimize bending loads. The tests were performed at room temperature and with a cross-head speed of 0.002 mm/sec. Postfracture analysis was performed by scanning electron microscopy and metallographic techniques.

⁶F. Padilla, W. C. Harrigan, Jr., and M. F. Amateau, Handbook of Test Methods for Evaluation and Qualification of Aluminum-Graphite Composite Materials, TR-0075(5621)-3, The Aerospace Corporation, El Segundo, California (21 February 1975).

III. PROCESSING EFFECTS

Five different processing methods were examined, four of which (S, H, C, and N) were used to produce the T 50/201 composite. Attempts to produce this same composite by the nickel-coating process were not successful because of the tightly twisted plies of the T 50 fiber, which prevented complete penetration by the nickel ions. Excellent penetration and plating adhesion was achieved with the HM 1000 high-modulus PAN fiber. This fiber is similar to the HM 3000 fiber except that it contains 1000 filaments/strand instead of 3000. The HM 1000/201 (P) composite was therefore substituted for the T 50/201 (P) originally intended. Two processing methods, S and C, were also examined for the composites produced with the T 300 fiber.

The strength and fracture appearance of these composites are summarized in Table 3. The percentage of theoretical strength of the precursor wire achieved by the various processes is included in this table to account for the differences in fiber fraction. A moderate improvement in longitudinal composite tensile strength is achieved by the application of the pyrolytic carbon coating to the T 50 fiber. This improvement may result from either the improved fiber fracture strength, caused by the healing of surface flaws, or from the additional layer of oriented carbon, which limits fiber matrix interaction. A combination of these processes may also be responsible for the improvement. The sodium process results in a composite with a lower absolute longitudinal strength because of the lower fiber fraction achieved by this process. Degradation of the fiber strength must also be contributing to the low composite strength since there is a reduction in the theoretical strength. It is evident from this table that transverse strength is greater for the T 50/201 composites with lower longitudinal strength. The appearance of the transverse fracture surface, as revealed by scanning electron microscopy, is also different for the various processing methods. A typical

Table 3. Transverse Strength and Fracture Behavior of Graphite-Aluminum Composites Processed by Various Methods

Composite and Processing Method	Precursor Wire Longitudinal Tensile Strength, MPa	Tensile Strength, % theoretical	Plate Transverse Tensile Strength, MPa	Occurrence of Fiber Pullout
T 50/201 Standard Ti-B CVD (S)	743	84	24.4	Slight
T 50/201 Hydrogen cleaning prior to CVD (H)	763	82	21.0	Moderate
T 50/201 Pyrolytic carbon prior to CVD (C)	920	94	19.0	Excessive
T 50/201 Sodium process (N)	407	66	43.2	None
HM 1000/201 Nickel-coated fibers (P)	138	34	27.8	Moderate
T 300/201 Standard Ti-B CVD (S)	212	19	55.8	None
T 300/201 Pyrolytic carbon prior to CVD (C)	1131	92	10.3	Excessive

transverse fracture surface of the T 50/201 (S) composite is shown in Fig. 4. The significant features of this fracture surface are the predominance of areas in which the matrix is stripped from the fiber, leaving the fiber surfaces clean, and the presence of fractured tensile ligaments consisting of either matrix and fibers or just matrix. Although the bulk of the matrix appears to be ductile, there is evidence of a brittle layer next to the fibers. This layer (Fig. 5) may be the product of the fiber-matrix reaction, e.g., aluminum carbide (Al_4C_3), or the product of the reaction between the titanium and boron coating and either the fiber or matrix, e.g., titanium carbide, boron carbide, or titanium aluminide. There is also some indication that these layers may contain oxides.⁷ The identification and exact nature of these reaction products are a subject for future publication. In spite of this brittle layer adjacent to the fibers, there is a general scarcity of fibers that are pulled out of the matrix from the tensile ligaments. This low incidence of fiber pullout indicates that there is some degree of fiber-matrix bonding; this bonding is quite minimal, however, since no aluminum adheres to the fiber surface.

A fracture surface very similar to that of the T 50/201 (S) composite is exhibited by the T 50/201 (H) composite, in which the fiber was first treated in hydrogen at 700°C before the standard coating treatment was applied. The main difference between the two materials is the amount of fiber pullout associated with the tensile ligaments. The T 50/201 (H) has slightly less transverse strength than the T 50/201 (S). The increase in the amount of fiber pullout is consistent with the decrease in fiber strength, although the slightly higher fiber fraction for the T 50/201 (H) may be the cause of the lower transverse strength.

⁷D. L. Dull and M. F. Amateau, Transverse Strength Properties of Graphite-Aluminum Composites, Quarterly Progress Report No. 2, TOR-0077(2726-03)-2, The Aerospace Corporation, El Segundo, California (10 April 1977).

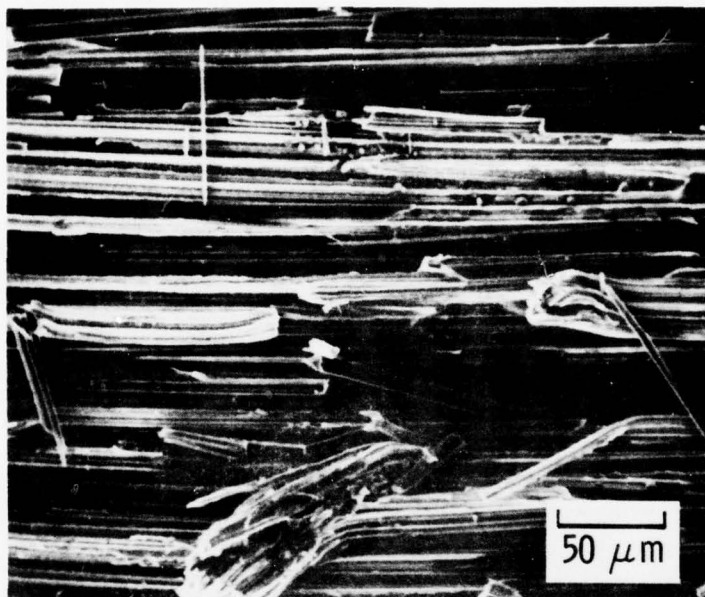


Fig. 4. Transverse Fracture Surface of
T 50/201 (S) Composite

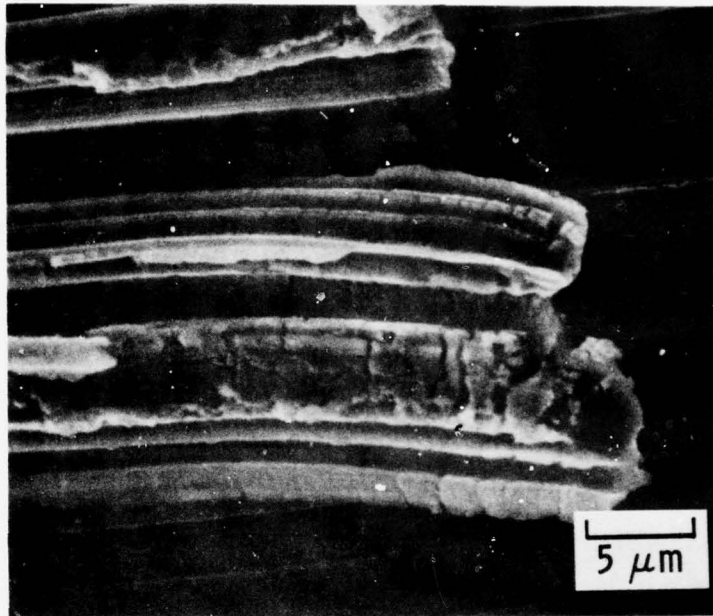
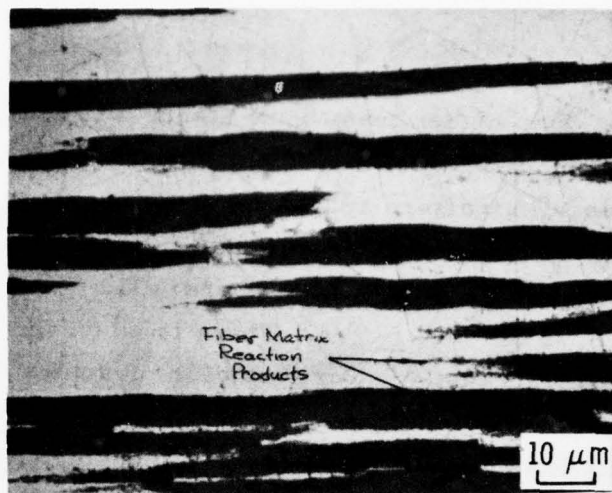


Fig. 5. Brittle Layer Attached to Ductile Aluminum Matrix

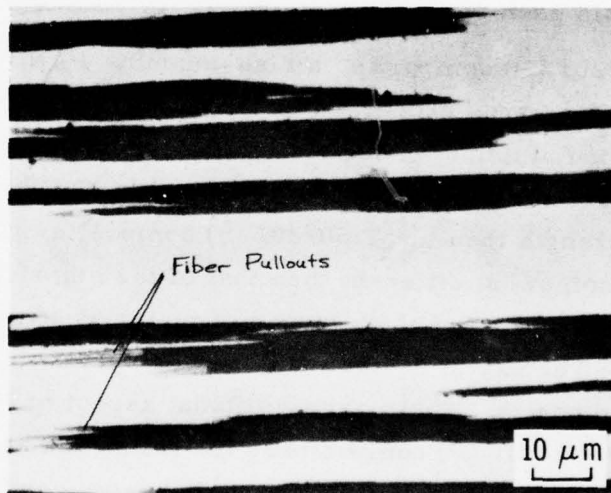
The T 50/201 (C) composites, in which the T 50 fiber is coated with pyrolytic carbon prior to the standard CVD treatment, have considerably greater amounts of fiber pullout, both throughout the fracture surface and in the tensile ligaments, than do the T 50/201 (S) or the T 50/201 (H) composites. The extent of fiber pullout in the T 50/201 (C) composite appears to be consistent with this composite's transverse fracture strength, which is lower than that of T 50/201 composites processed by the other two CVD coating methods. At present, it is not clear why the hydrogen pretreatment of the fiber should result in either lower transverse strength (if this indeed is not a volume-fraction effect) or more extensive fiber pullouts. On the other hand, the influence of the pyrolytic carbon interface on transverse strength (neglecting the possible fiber-fraction effect) and fracture appearance is more easily explained in terms of the degree of fiber-matrix interaction. As is evident in Table 2, there was significantly less aluminum carbide formation in the T 50/201 (C) than in either the T 50/201 (S) or T 50/201 (H).

Although the degree of fiber-matrix reaction in the various T 50/201 composites was not conspicuous, it was evident when metallographic examination was performed at magnifications to 1000X. Longitudinal metallographic sections of composites with no fiber-matrix interaction and some fiber-matrix interaction are shown in Fig. 6. In the T 50/201 (S) composite, Fig. 6a, fine precipitates can be seen along the edge of the fibers and especially near the areas where the fibers bend beneath the surface of aluminum. Note the absence of these precipitates in the T 50/201 (C) composite of Fig. 6b. Areas where the fiber has been pulled out of the matrix in the T 50/201 (C) composite are also evident in this figure. In the longitudinal metallographic sections, the amount of fiber pullout resulting from metallographic specimen preparation was consistent with the degree of fiber pullout found on the transverse fracture surfaces.

The transverse strength of the T 50/201 (N) composite, produced by the sodium process, is significantly higher than that of composites produced



T 50/201 (S)
a.



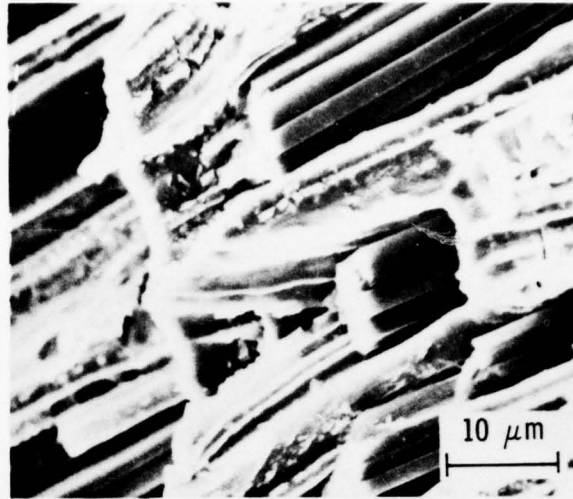
T 50/201 (C)
b.

Fig. 6. Longitudinal Metallographic
Sections of T 50/201
Composites

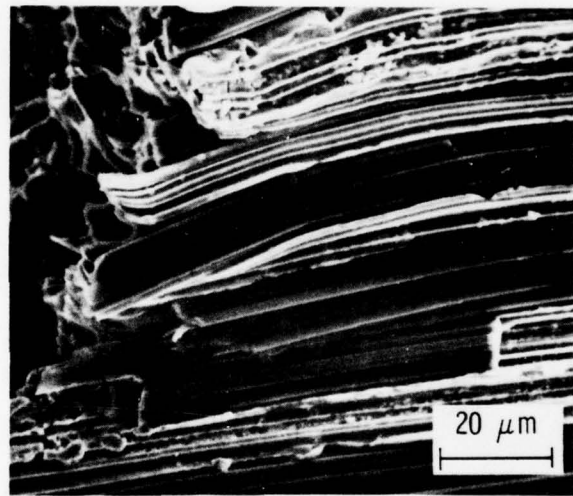
by the CVD process. This higher transverse strength is consistent with differences in the fracture appearance of the T 50/201 (N) (Fig. 7). However, the difference in fracture appearance may be due, in part, to the much lower fiber fraction in the sodium-processed composite. The T 50/201 (N) has less than 15-vol% fibers, whereas the CVD-processed composite has more than 30-vol% fibers. There is no evidence of fiber pullout on tensile ligaments or other portions of the fracture surface in this composite. No longitudinally split fibers were found, although there were some transverse cracks in the fiber as a result of bending (Fig. 7). A considerable amount of matrix ductility is also characteristic of the transverse fracture of this composite. No material appears to adhere to the fibers, as indicated in each photomicrograph of Fig. 7.

The HM 1000/201 (P) composite, a high-modulus PAN fiber in the form of 1000 filament strands processed by nickel plating and subsequent immersion into molten aluminum, has a slightly higher transverse fracture strength than the T 50/201 composite processed by the CVD method but a lower transverse strength than the T 50/201 (S) composite. The fracture appearance is also somewhat different than that of the other composites. Although no fiber splitting was found, pieces of material adhered to many of the exposed fibers. The extent of fiber pullout was very similar to that for the T 50/201 (H) composite. The most significant aspect of the fracture surface of the HM 1000/201 (P) composite is the numerous areas of brittle matrix fracture. An example of brittle matrix behavior can be seen in Fig. 8. This behavior, of course, was not unexpected in view of the likelihood of nickel aluminide formation during the infiltration process. The relatively high transverse strength in this composite may be a result of the low fiber fraction rather than of any enhancement of fiber-matrix bonding.

Evidence of aluminum-nickel intermetallic compounds formed and the low concentration of graphite fibers in this composite can be seen in Fig. 9.



TENSILE LIGAMENT PORTION OF TRANSVERSE FRACTURE
a.



TRANSVERSE CRACKING DUE TO FIBER BENDING
b.

Fig. 7. Transverse Fracture Surface of
Sodium-Processed T 50/201 (N)
Composite

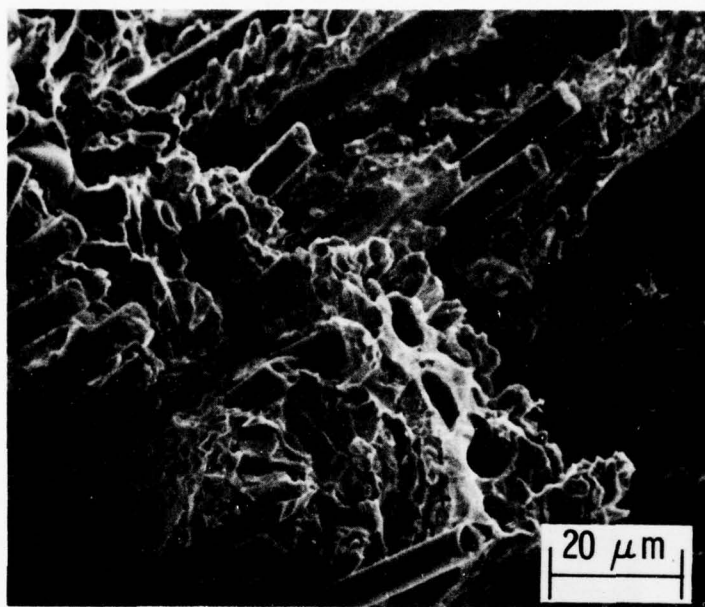
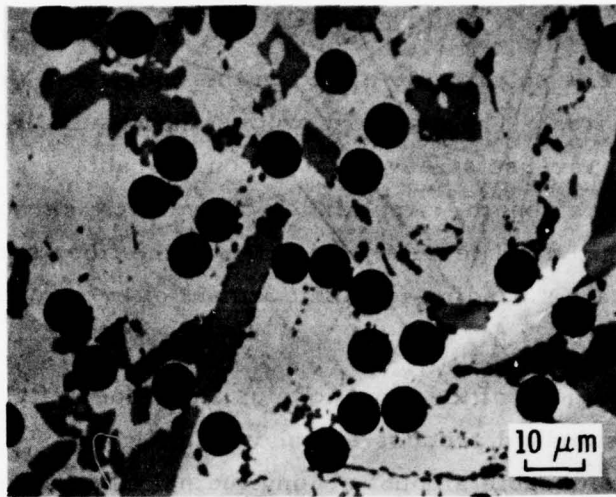


Fig. 8. Fracture Surface of HM 1000/201
(P) Composite



TRANSVERSE VIEW
a.



LONGITUDINAL VIEW
b.

Fig. 9. Longitudinal and Transverse
Sections of HM 1000/201 (P)
Composite

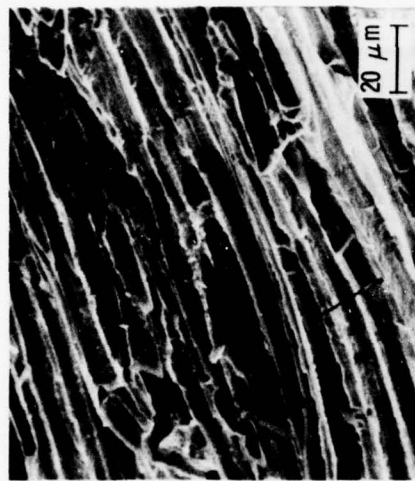
Processing has an extreme effect on the transverse strength of the T 300/201 composites. The standard processing results in a dramatic increase in the transverse strength but in considerable degradation of the longitudinal tensile strength. Application of pyrolytic carbon to the T 300 preserves the longitudinal tensile properties of the fiber but does not permit sufficient fiber-matrix bonding for achievement of even moderate transverse strength.

Fracture surfaces of the low-modulus PAN-based fiber infiltrated with aluminum by the standard process are shown in Fig. 10. The most distinctive feature is the considerable amount of longitudinal fiber splitting (Fig. 10a). The fracture patterns on the fibers can also be seen on the matrix (Fig. 10b). Bending of tensile ligaments produced a profusion of transverse cracks on the fiber with very little evidence of fiber pullout (Fig. 10c). Although there is some matrix ductility in this composite, there appears to be less ductility than in the other composites (Fig. 10d). The high carbide concentration found in these composites may be responsible for this effect. In those areas where fiber splitting did not occur extensively, a considerable amount of material adheres to the fiber surface (Fig. 11).

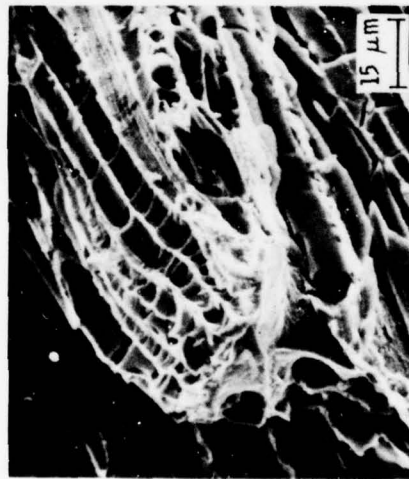
In the T 300/201 composite produced by applying a pyrolytic carbon coating to the fiber, there was a significant modification in the fracture surface appearance. Fiber splitting was totally absent, with only a modest amount of transverse cracking where the fibers remain embedded in the matrix. For the most part, the fiber surfaces were stripped clean during fracture (Fig. 12); occasionally, however, some bulk matrix material or a thin coating adhered to a fiber (Fig. 13). An unusually large amount of fiber pullout (Fig. 14) was quite characteristic of the transverse fracture surface of this composite. The large number of ductile tensile ligaments is consistent with the general impression of very poor fiber-matrix bonding in these fractographs.



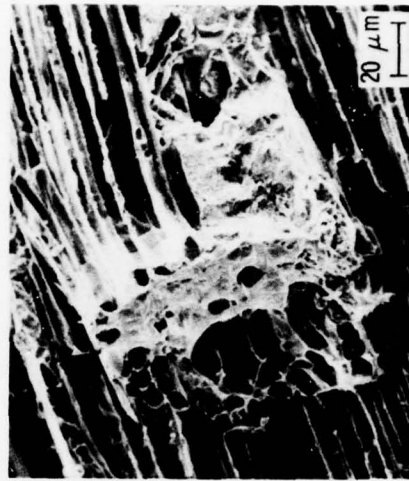
FIBER SPLITTING
a.



FRACTURE PATTERNS
b.



TRANSVERSE FIBER CRACKING
c.



MINIMUM DUCTILITY IN LIGAMENT
d.

Fig. 10. Fracture Surfaces of T 300/201 (S) Composite

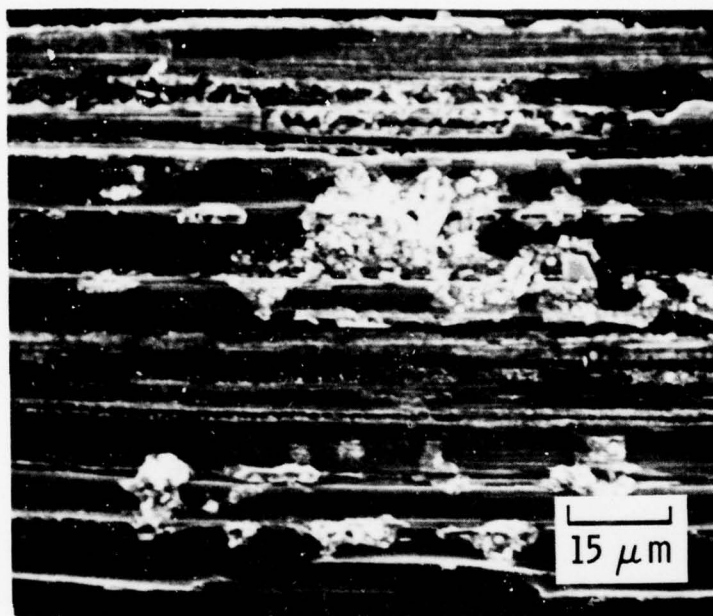


Fig. 11. Adherence of Material to Surface
of Fiber on T 300/201 (S)
Fracture Surface

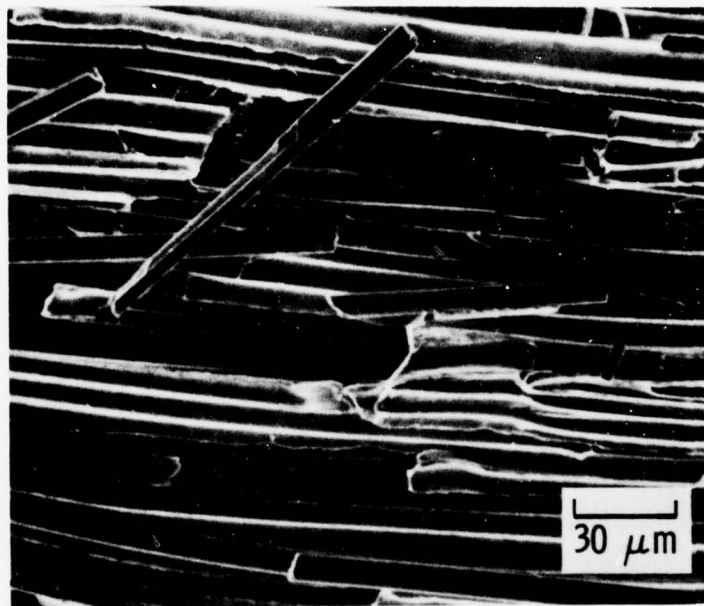


Fig. 12. Clean Appearance of Fibers on
T 300/201 (C) Fracture Surface

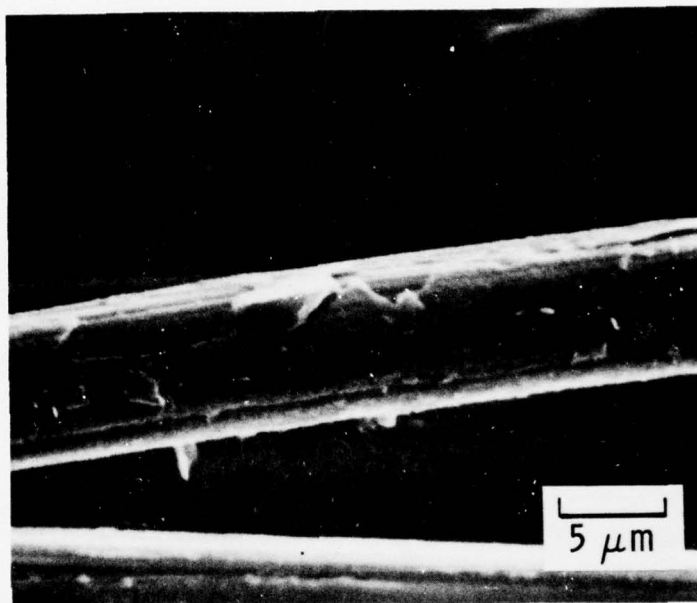


Fig. 13. Coating on T 300 Fibers Pulled
From T 300/201 (C) Fracture
Surface

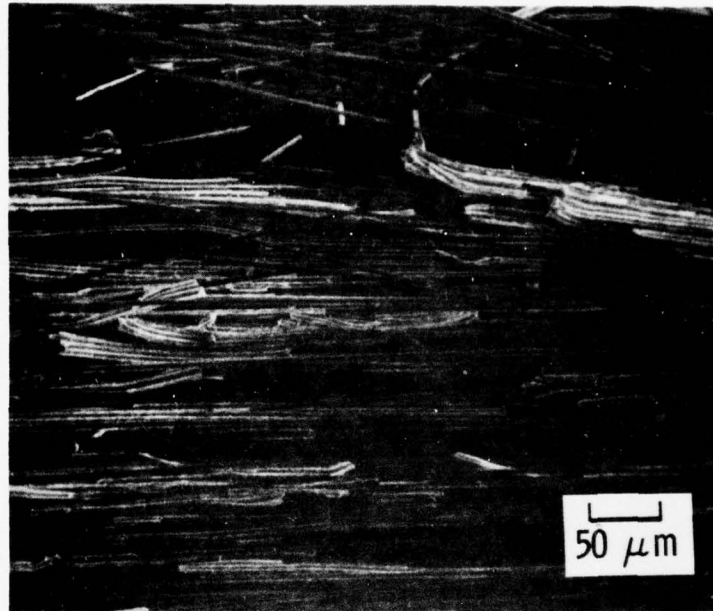
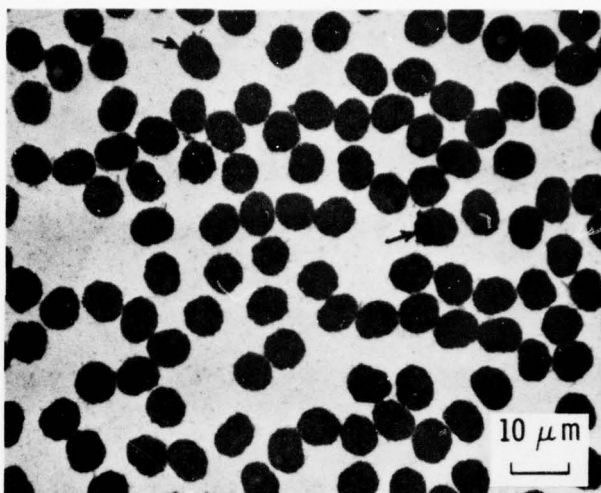
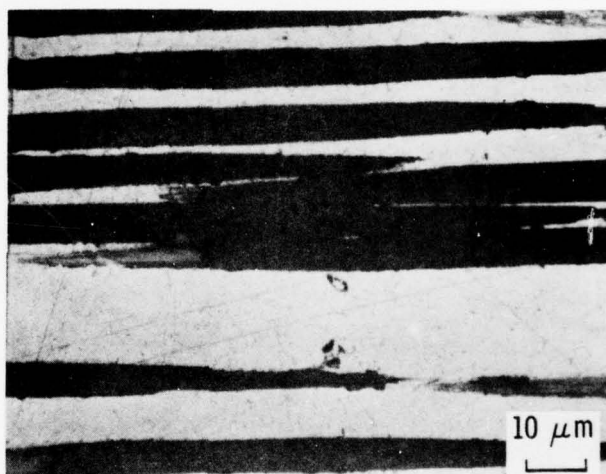


Fig. 14. Fiber Pullout on T 300/201 (C)
Fracture Surface

Limited fiber matrix bonding was also evident in the metallographic sections of T 300/201 composites produced by the S and C processes. In addition to the fiber pullouts that were evident in the longitudinal sections of the T 300/201 (C) composite, there were also separations between the fiber-matrix interface in the transverse sections. These features, shown in Fig. 15, were not found in the T 300/201 (S) composites.



FIBER-MATRIX CRACKS IN TRANSVERSE VIEW
a.



FIBER PULLOUT IN LONGITUDINAL VIEW
b.

Fig. 15. Longitudinal and Transverse
Sections of T 300/201 (C)
Composite

IV. FIBER AND MATRIX EFFECTS

In the 201 matrix alloy composite, differences in transverse strength and fracture behavior occurred with fibers other than the T 50 and T 300. A summary of the composite strength and fracture appearance of the composites produced with the Type P and HM 3000 fibers, as well as with the T 50 and T 300 fibers, is given in Table 4. The transverse strength of the Type P/201 (S) composite was somewhat greater than that of the T 50/201 (S) composite. This is in agreement with the appearance of the fracture surface of the Type P/201 (S) composite, which indicated that some degree of fiber-matrix bonding had occurred. Fiber splitting was observed in these composites, especially in the "wedge-missing" -shaped fibers. Fiber pullout was also limited, and a considerable amount of matrix material adhered to the surface of the fibers.

The HM 3000 fiber had the poorest transverse strength of all the 201 matrix composites processed by the S method. Fiber pullout was quite noticeable on the fracture surfaces. The fiber surfaces on the fracture were quite smooth and generally free of adhering material (Fig. 16).

The differences in transverse strength of the four different fibers could be the result of a combination of effects. The fiber-matrix reaction involving the formation of Al_4C_3 appears to follow the trend in transverse strength for each of the composites (Fig. 17).

The shape of the fiber may also have an effect on the transverse fracture strength of the composite. Fibers that have irregular cross sections, such as T 50 and Type P, should provide some mechanical locking with the matrix, thus enhancing transverse strength. Of the four fibers used in this study, the HM 3000 fiber, which is almost perfectly circular and contains no surface striations, offers the least in the way of mechanical locking.

Preceding Page BLANK

Table 4. Effect of Fiber Type on Transverse Strength and Fracture Behavior of Graphite/201 Matrix-Alloy Composites Processed by Standard Ti-B CVD Method (S)

Fiber	Longitudinal Tensile Strength, MPa	Strength, % theoretical	Transverse Tensile Strength, MPa	Occurrence of Fiber Pullout
Thornel 50 (T 50)	743	84	24.4	Slight
Thornel 300 (T 300)	212	19	55.8	None
Thornel Type P (Type P)	313	61	28.9	Slight
Hercules HM 3000 (HM 3000)	1014	98	11.1	Moderate

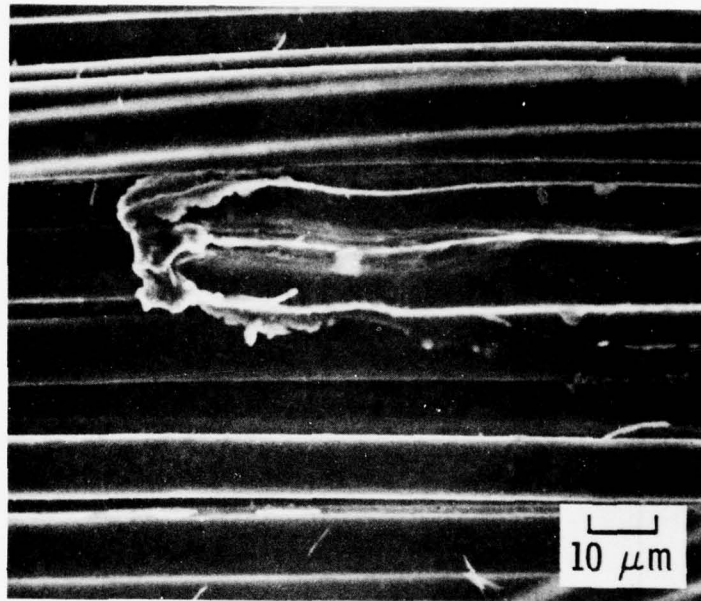


Fig. 16. Fracture Surface of HM 3000/201 (S) Composite

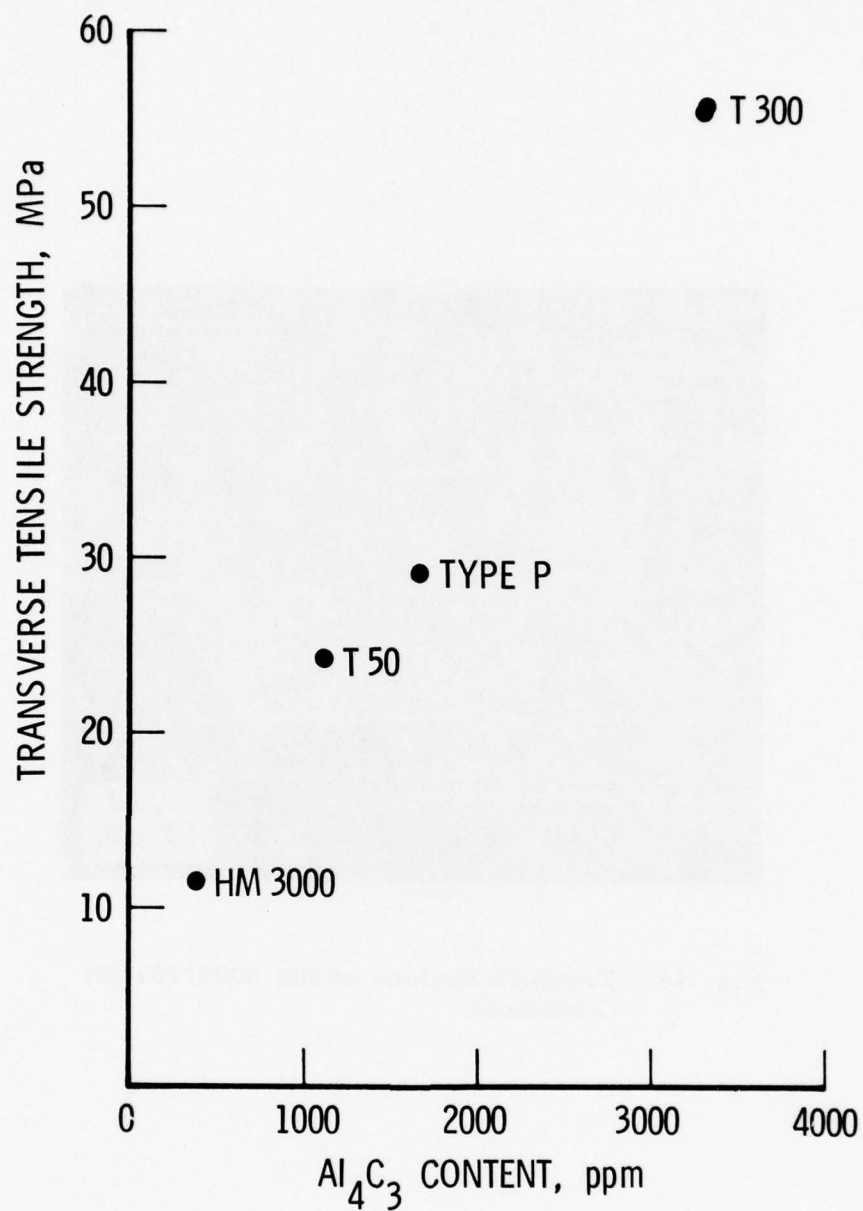


Fig. 17. Relationship Between Carbide Formation and Transverse Strength of Various Graphite Fiber/201 (S) Composites

The effect of matrix-alloy composition on the transverse strength and fracture behavior of HM 3000 fiber composites produced by the S process is given in Table 5. There is practically no difference in transverse strength for the three composites listed. The amount of fiber-matrix reaction of the three composites is quite low, as indicated by the Al_4C_3 content. The effect of matrix alloy on the fracture appearance of HM 3000 fiber composites is also quite modest. There is virtually no difference in the transverse fracture appearance of the 6061 and 201 matrices. The 1100 alloy-matrix composite is also similar, but there appears to be slightly more fiber pullout than in the other matrix-alloy composites.

Table 5. Effect of Matrix-Alloy Composition on Strength and Fracture Behavior of HM 3000/Aluminum-Alloy Composites Produced by S Process

Aluminum Matrix Alloy	Longitudinal Tensile Strength, MPa	Transverse Tensile Strength, MPa	Occurrence of Fiber Pullout
201	1014	11.1	Moderate
6061	692	10.7	Moderate
1100	621	9.7	Excessive

V. THERMAL TREATMENTS

The transverse strength of graphite-aluminum composites appears to depend upon the amount of reaction between the fiber and the matrix. A series of heat treatments was performed on T 50/201 (S) composites at temperatures near the solidus of the matrix alloy in order to determine the effectiveness of thermal treatments in promoting fiber-matrix reactions. The primary reaction in this temperature range is the formation of aluminum carbide. Heat-treatment temperatures of 571 and 593°C were selected to be, respectively, nominally below and above the solidus temperature of the 201 aluminum alloy. The transverse strength and aluminum carbide content for the various thermal treatments are given in Table 6.

Table 6. Transverse Fracture Behavior of T 50/201 (S) Composite Heat Treated To Produce Additional Fiber-Matrix Reaction

Heat Treatment Time, hr	Temperature, °C	Transverse Strength, MPa	Al ₄ C ₃ Content, ppm	Occurrence of Fiber Pullout
	None	24.4	1,012	Slight
4.5	571	15.1	1,121	Slight
4.5	593	21.3	7,858	Slight
24	571	32.5	>10,000	None
24	593	27.3	>10,000	None
48	571	33.0	>10,000	None
48	593	34.0	>10,000	None

Thermal treatments at either 571 or 593°C for 4.5 hr result in an initial decrease in transverse strength, followed by an increase in strength

for longer treatment times. This decrease in transverse strength coincides with a softening of the matrix alloy (Fig. 18). After the first 4.5 hr, the amount of additional matrix softening is slight. The carbide content for the 571°C treatment remains essentially unchanged, whereas that for the 593°C treatment increases significantly. This difference in the degree of carbide formation may explain the less pronounced drop in transverse strength after 4.5 hr for the 593°C treatment than for the 571°C treatment. At 24 hr and longer, the carbide content increases significantly, resulting in the increased transverse strength.

Significant differences in the fracture surfaces of T 50/201 (S) composites after they have been given high-temperature thermal treatments have also been observed. T 50/201 (S) specimens heated for 4.5 hr at 571 or 593°C had the same fracture appearance as the untreated specimen, i.e., clean fiber surfaces and the absence of longitudinal splitting (Fig. 19). Heating the specimens to 24 hr at these temperatures resulted in extensive longitudinal fiber splitting (Fig. 20a) and transverse cracking, with almost no fiber pullout (Fig. 20b). In addition, a considerable amount of material adhered to the surfaces of exposed fibers of fractured specimens heat treated for 24 hr. Heating the specimens for 48 hr resulted in a transverse fracture appearance very similar to that after the 24-hr treatment. Longitudinal fiber splitting was so extensive in these specimens that splitting in two planes was occasionally observed (Fig. 21). The extent of the fiber-matrix reaction can be seen in the longitudinal cross-sectional view of Fig. 22. After 4.5 hr at 571°C (Fig. 22a), there is no evidence of fiber-matrix interaction, and the microstructure is quite similar to that of the composite that was not heat treated (Fig. 7a). The precipitates or reaction products after 48 hr of treatment at 571°C are quite evident in Fig. 22b. Transverse sectional views of the composites after 4.5 and 48 hr of heat treatment at 571°C are shown in Fig. 23. After 4.5 hr, there was very little attack on the fiber surfaces (Fig. 23a); after 48 hr, however, the outer surfaces of the fibers were attacked to the extent that the sharp crenulated surfaces were obliterated (Fig. 23b). The 48-hr treatment results in a decrease in

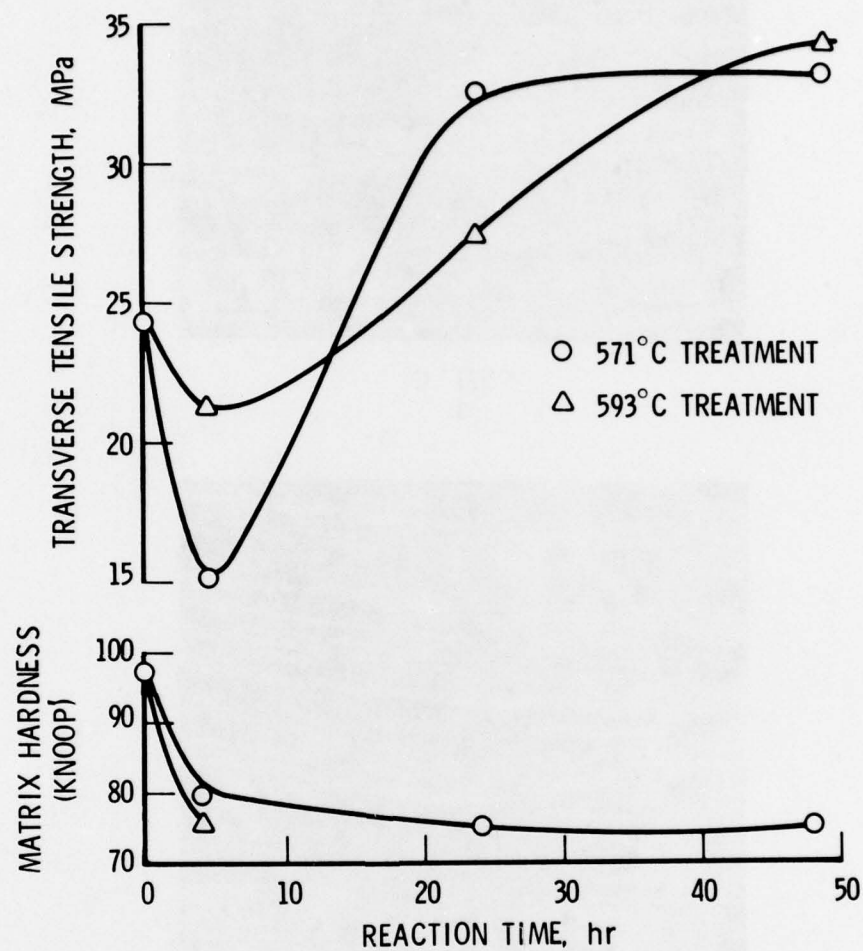
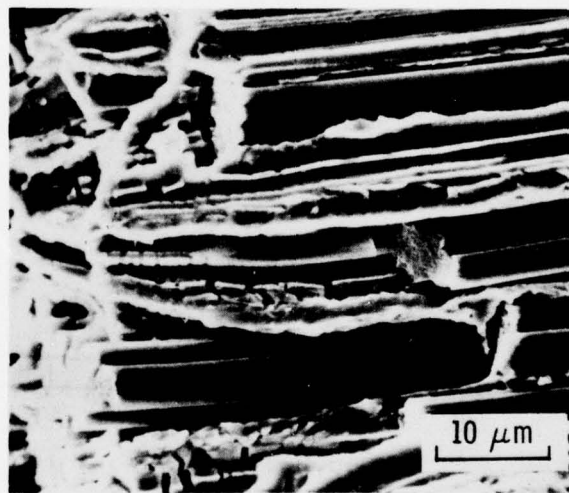


Fig. 18. Effect of Thermal Treatments on Transverse Strength and Matrix Hardness of T 50/201 (S) Composite

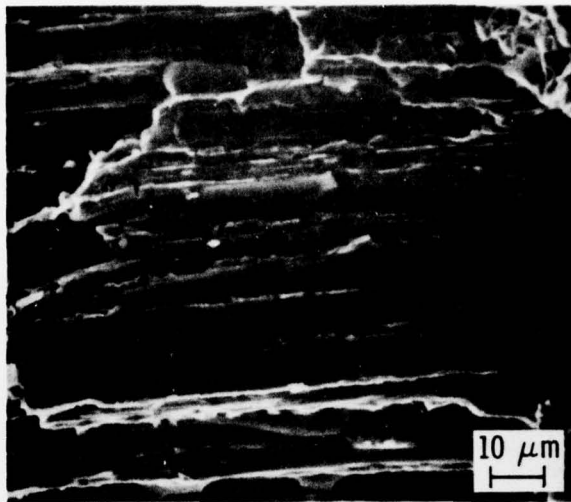


571° C
a.

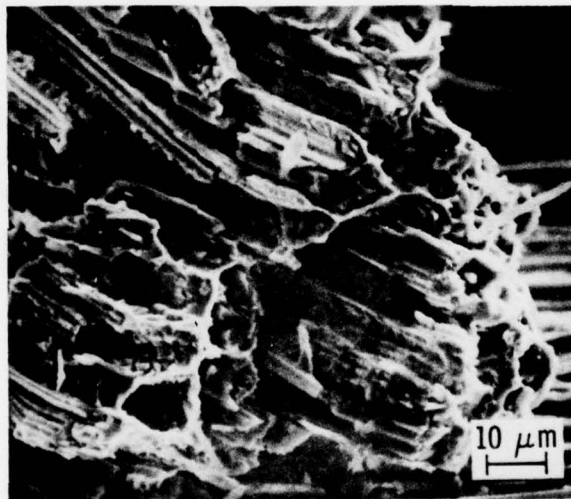


593° C
b.

Fig. 19. Fracture Surface of
T 50/201 (S) Composite
Heat Treated Near
Solidus Temperatures
for 4.5 hr



593°C
a.



571°C
b.

Fig. 20. Fracture Surface of T 50/201 (S)
Composite Heat Treated Near
Solidus Temperature for 24 hr

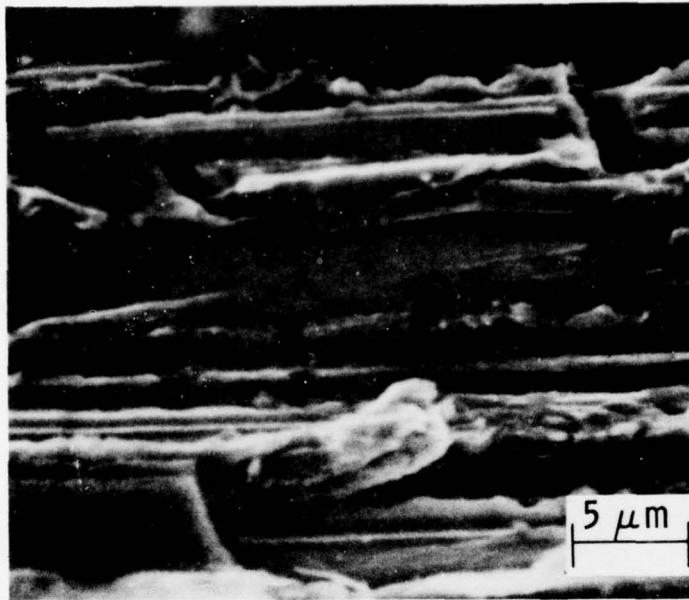
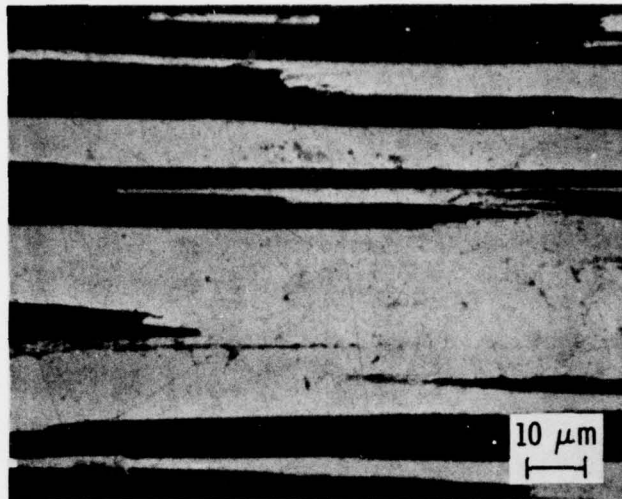
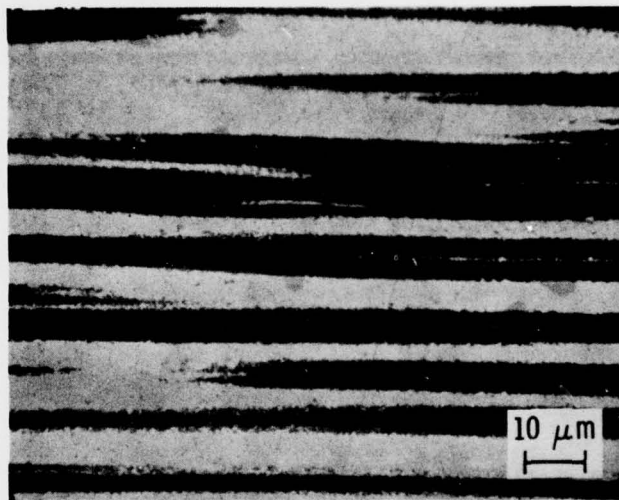


Fig. 21. Longitudinal Fiber Splitting in
T 50/201 (S) Composite Heat
Treated at 571°C for 48 hr

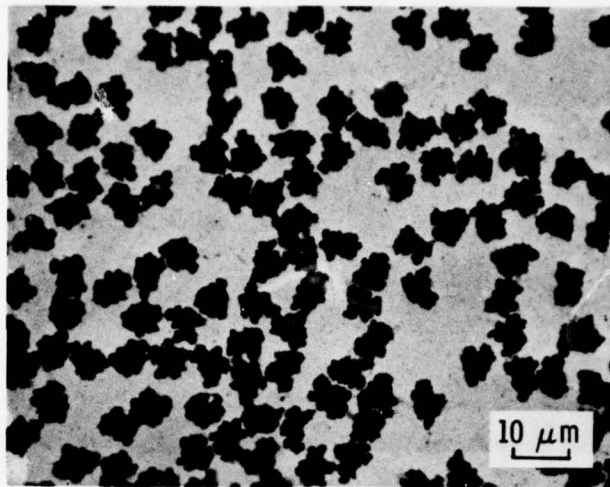


4.5 hr
a.

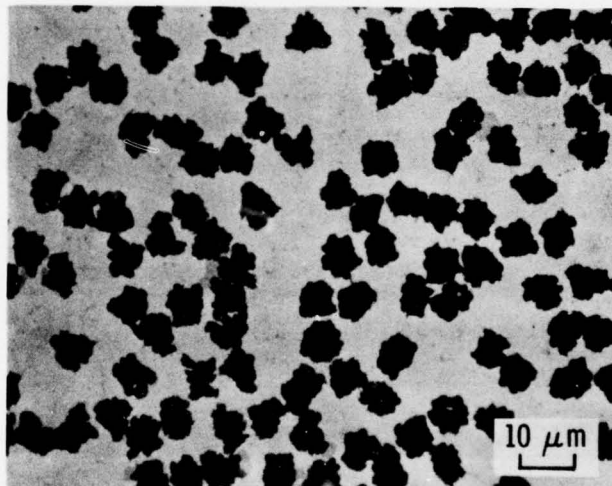


48 hr
b.

Fig. 22. Longitudinal Cross Section of
T 50/201 (S) Composite Heat
Treated at 571°C



4.5 hr
a.



48 hr
b.

Fig. 23. Transverse Cross Section of
T 50/201 (S) Composite Heat
Treated at 571°C

fiber volume fraction from about 0.32 to 0.29. This loss in fiber cross section, as well as the degradation of the fiber surface smoothness, probably results in an unacceptable decrease in longitudinal strength in spite of the slight increase in transverse strength.

VI. FIBER FRACTION AND DISTRIBUTION

Processing the graphite-aluminum composite by different methods results in some differences in transverse strength; however, each processing method also results in a different and characteristic fiber fraction. Unequivocal separation of fiber-fraction effects from true-bond strength effects is not possible at the present time. In general, as the fiber fraction increases, the transverse strength is expected to decrease, since the fiber-matrix bond is probably low compared with the matrix-matrix bond or even with the transverse fiber strength. However, in addition to the effect of fiber fraction, the transverse strength is expected to be significantly influenced by the arrangement or local concentration of the fibers. An examination of the mechanism of transverse fracture indicates that the preferred fracture path is in areas of heavy fiber concentration (Ref. 3). Thus, if the processing method results in continuous matrix paths in the direction of the load, the areas of high fiber concentration contribute little to the load bearing area. The gross transverse strength will then increase as these areas make up less of the total cross section. If, on the other hand, the areas of high fiber concentration form a continuous path normal to the transverse direction, the transverse strength may be independent of overall fiber concentration but dependent on the local fiber concentration. This situation is illustrated in Fig. 24, in which absolute fiber fraction is plotted against strength, without regard to processing method or local fiber concentrations. The data points for the HM 3000/6061 (S) composite that lay near the solid curve are for samples in which the fiber fraction was intentionally varied; this was accomplished by diluting the precursor wire (normally 30% to 35% fibers) with pure matrix wires during consolidation in a way that resulted in continuous paths of matrix parallel to the transverse loading direction. The decrease in transverse strength with increasing fiber fraction is quite evident. One specimen that contained only 11% fibers had a transverse strength very

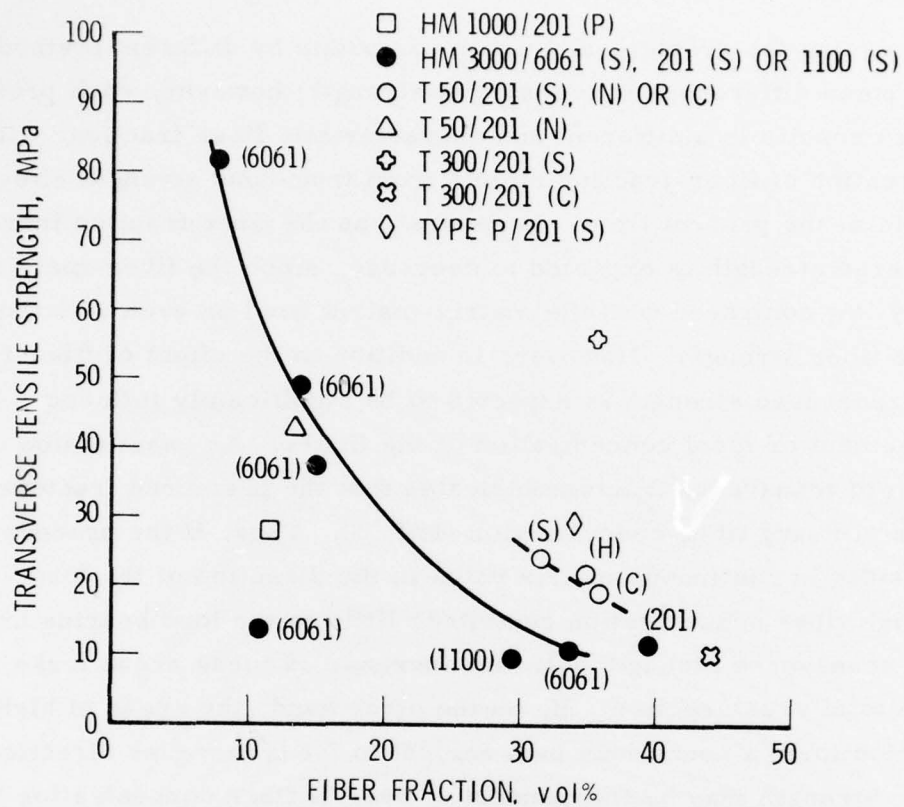


Fig. 24. Composite Fiber Fraction Versus Transverse Strength, Plotted Without Regard to Processing Method or Local Fiber Concentrations

similar to that of the composite with 30% to 35% fiber fraction. This composite had continuous paths of 30% to 35% fiber areas normal to the transverse loading direction.

In view of these effects, the difficulty in determining the intrinsic bond strengths on the basis of transverse strength values alone can be appreciated, since the local concentration of fibers cannot be completely documented. Therefore, to some extent, the qualitative and hence subjective criteria of fracture appearance must be used as an aid in the assessment of bond strength. However, in an attempt to arrive at general conclusions regarding intrinsic bond strength from the transverse values alone, it is reasonable to compare composites with more or less uniform fiber distributions and with similar fiber fractions, e.g., within a range from 5% to 10%. The composites that can be compared on this basis fall into two groups: one of low fiber fraction and one of higher volume fraction (Fig. 24). The low-volume fraction group consists of T 50/201 (N) and HM 1000/201 (P). The high-volume fraction group includes the remaining composites studied.

VII. CONCLUSIONS

With the limitations imposed by the uncertainties of the composite structure and volume fraction effects taken into account, the following conclusions are offered:

1. Of the T 50/201 composites produced by the CVD process, the S process results in the highest transverse strength and the greatest degree of fiber-matrix reaction. The transverse strength and degree of fiber pullout seem to be inversely related.
2. For the T 300/201 composites, there are marked differences in transverse strength and fracture appearance between the S- and C-processed composites. The S process results in high transverse strength and longitudinal fiber splitting, whereas the C process results in low transverse strength and excessive fiber pullout.
3. Of the low fiber fraction composites, the sodium-processed composite has greater transverse strength than does the nickel-plated fiber composites. The P process also produces a brittle matrix.
4. The transverse strength of the composites is also related to the degree of reaction between the fiber and the matrix. The T 300, which reacts most extensively with the aluminum alloys, has the greatest transverse strength, followed by Type P, T 50, and HM 3000.
5. The transverse strength seems to be only slightly influenced by matrix composition.
6. Thermal treatments that promote fiber-matrix reactions can increase transverse strength but do so at the sacrifice of fiber integrity.

Preceding Page BLANK

THE IVAN A. GETTING LABORATORIES

The Laboratory Operations of The Aerospace Corporation is conducting experimental and theoretical investigations necessary for the evaluation and application of scientific advances to new military concepts and systems. Versatility and flexibility have been developed to a high degree by the laboratory personnel in dealing with the many problems encountered in the nation's rapidly developing space and missile systems. Expertise in the latest scientific developments is vital to the accomplishment of tasks related to these problems. The laboratories that contribute to this research are:

Aerophysics Laboratory: Launch and reentry aerodynamics, heat transfer, reentry physics, chemical kinetics, structural mechanics, flight dynamics, atmospheric pollution, and high-power gas lasers.

Chemistry and Physics Laboratory: Atmospheric reactions and atmospheric optics, chemical reactions in polluted atmospheres, chemical reactions of excited species in rocket plumes, chemical thermodynamics, plasma and laser-induced reactions, laser chemistry, propulsion chemistry, space vacuum and radiation effects on materials, lubrication and surface phenomena, photo-sensitive materials and sensors, high precision laser ranging, and the application of physics and chemistry to problems of law enforcement and biomedicine.

Electronics Research Laboratory: Electromagnetic theory, devices, and propagation phenomena, including plasma electromagnetics; quantum electronics, lasers, and electro-optics; communication sciences, applied electronics, semiconducting, superconducting, and crystal device physics, optical and acoustical imaging; atmospheric pollution; millimeter wave and far-infrared technology.

Materials Sciences Laboratory: Development of new materials: metal matrix composites and new forms of carbon; test and evaluation of graphite and ceramics in reentry; spacecraft materials and electronic components in nuclear weapons environment; application of fracture mechanics to stress corrosion and fatigue-induced fractures in structural metals.

Space Sciences Laboratory: Atmospheric and ionospheric physics, radiation from the atmosphere, density and composition of the atmosphere, aurorae and airglow; magnetospheric physics, cosmic rays, generation and propagation of plasma waves in the magnetosphere; solar physics, studies of solar magnetic fields; space astronomy, x-ray astronomy; the effects of nuclear explosions, magnetic storms, and solar activity on the earth's atmosphere, ionosphere, and magnetosphere; the effects of optical, electromagnetic, and particulate radiations in space on space systems.

THE AEROSPACE CORPORATION
El Segundo, California